Short- and long-term velocity variations and strain evolution at Ischia (ITALY) and their implications for dynamics of the hydrothermal system

Stefania Tarantino[1*], Piero Poli[2], Maurizio Vassallo[1], Nicola D'Agostino[1]

[1]Istituto Nazionale di Geofisica e Vulcanologia, Italy

[2]Department of Goescience, University of Padova, Padova, Italy

*Corresponding author

E-mail address: stefania.tarantino@ingv.it (S. Tarantino)

Key Points:

- We characterise short and long-term seismic wave velocity variations during 8 years at the volcanic Island of Ischia (Italy).
- We revealed a significant coseismic drop in occurrence of the 2017 M_w 3.9 Casamicciola earthquake tracking the near-surface damage.
- We observe a remarkable sensitivity of the seismic wave velocity to depressurization processes of the hydrothermal system.

Abstract

In active volcanic systems, the elevated pressurization of fluids and the movement of melt materials have an enormous influence on the stress-state of rocks and their mechanical behavior. We use seismic ambient noise to evaluate the static seismic velocity variations related to long-term volcanic deformation, and the dynamic changes associated with the 2017 Casamicciola earthquake (M_w 3.9), in the active volcanic complex of the Ischia Island (Italy). Our study reveals a significant dynamic velocity reduction (~0.2%) mostly related to the near-surface damage, with a permanent drop near the red zone, that we posit to be related to the documented landslides and the subsidence observed immediately after the earthquake. We also report a positive long-term linear trend of velocity variations, sensitive to a generalized contraction of the Ischia Caldera that we revealed with geodetic modeling. Our results suggest a depressurization of the shallow hydrothermal system, through degassing along faults or sills.

Plain summary Language

Volcanic rocks experience a wide range of phenomena characterized by complex and fast-paced dynamics, spanning from elevated geothermal gradients and convoluted stress patterns to pressurization/depressurization of fluids of heterogeneous composition, possibly with more thermodynamic phases. In this study, we use relative seismic wave velocity measurements from Coda Wave Interferometry and Global Positioning System measurements to show that velocity variations are extremely sensitive to depressurization processes, coseismic dynamic strains and level of damage, when distinguished from seasonal variations related to underground infiltration of rainwater. The sensitivity of velocity changes to dynamic stress perturbations is generally considered a proxy of the level of pressurization of the hydrothermal and/or magmatic fluids in volcanic areas. Our findings reflect a heterogenous shallow degassing, mostly effective in the northern part of the Island, and a reduced effective stress in the southern part, where a higher geothermal gradient and a more intense hydrothermal activity are present, characterized by highly pressurized fluids. While geodetic measurements are limited to the surface, seismic velocity variations enclose information on the interior of the crust. Their integrated use enables the characterization of deformation processes at different depth ranges, which is pivotal for the monitoring of the magmatic systems.

Introduction

Volcanic systems undergo intricate deformations associated with the dynamics of deep magmatic systems, and their geodetic observation at the surface provides unique insights into the volcanic cycle (Caricchi et al., 2021; Segall, 2013; Snieder & Hagerty, 2004; Townsend, 2022). The rocks respond to these deformations by generating a complex strain field (Donaldson et al., 2019) and associated changes in the mechanical properties (Brenguier et al., 2016; Brenguier, Shapiro, et al., 2008; Rivet et al., 2014). These changes also lead to measurable variations in the seismic wave velocity (δv/v) (Brenguier, Shapiro, et al., 2008; Donaldson et al., 2019; Duputel et al., 2009; Rivet et al., 2014; Snieder & Hagerty, 2004). The δv/v can be correlated, for instance, with pre-eruptive stress buildup within the magmatic reservoir (Rivet et al., 2014) or with velocity drops (increases) sensitive to summit inflations (deflations) (Duputel et al., 2009; Makus et al., 2023). Moreover, by establishing a relationship between strain and δv/v through the definition of strain sensitivity (Jin et al., 2018; Ostrovsky & Johnson, 2001), it becomes possible to derive fundamental insights about the non-linear response of rocks and, consequently, assess their rheology (Delorey et al., 2021; Poli et al., 2020).

To date, the combined study of geodetic methods and seismic wave velocity changes has yielded profound insights into the physical processes in active magmatic systems (Cabrera-Pérez et al., 2023; Caudron et al., 2021, 2022; Cubuk-Sabuncu et al., 2021; Donaldson et al., 2017; Olivier et al., 2019; Rivet et al., 2014), but has also extended its contribution to fundamental understandings of the rheology of volcanic rocks (Takano et al., 2019). To name a few examples of successful integration of interdisciplinary data, in central Iceland, the correlation between relative velocity and volumetric strain in regions of both compression and dilatation has been associated with a dike intrusion, which was partially masked by superimposed seasonal cycles resulting from elastic and poroelastic responses to changing snow thickness, atmospheric pressure, and groundwater level (Donaldson et al., 2019). In SW Iceland, repeated crustal magmatic intrusions in a complex plate boundary zone and the concurrent opening of new cracks to accommodate magma propagation resulted in a co-intrusive seismic velocity reduction (Cubuk-Sabuncu et al., 2021). Thanks to the use of continuous seismic records and novel approaches, Caudron et al., (2021) revealed that an apparent quiescent period before a phreatic eruption at Mt Ontake was preceded indeed by an intriguing sequence of correlated seismic velocity and volumetric strain changes, starting months before the eruption and due to the dynamics of undetected pressurized fluids.

In this study, we investigate the velocity variation (δv/v) of the Ischia volcanic complex in response to quasi-static and dynamic strain perturbations, respectively associated with long-term volcanic deformation and local earthquakes (Calderoni et al., 2019; Galvani et al., 2021; Sepe et al., 2007; Trasatti et al., 2019) (Fig. 1). To achieve this objective, we employ ambient seismic noise interferometry to estimate δv/v at various seismic stations (N. M. Shapiro & Campillo, 2004). Concurrently, we quantify both static and dynamic strains through the utilization of a local GNSS network (De Martino et al., 2021) (see Fig. 1)

With our integrated approach, we untangled the significant short-term velocity reduction and permanent damage caused by small magnitude earthquakes impacting the shallow hydrothermal system, distinguishing it from a long-term velocity increase that connected with the depressurization of the shallow hydrothermal reservoir. Our multidisciplinary study highlights the possibility to decipher varied rock responses, contributing to elucidate the physical processes within the hydrothermal system and its connection to seismicity. This insight can further open new possibilities for monitoring the physical state of industrial geothermal sites.

The Ischia Volcanic complex

The study area (Fig. 1) encompasses the westernmost active volcanic complex of the Campanian plain, incorporating Campi Flegrei, Procida, and Vesuvius in Southern Italy (Civetta et al., 1991). A hydrothermal system subject to depressurization (Sepe et al., 2007) exists within the volcanic edifice of Ischia, causing subsidence (up to −15 ± 2.0 mm/yr) with a centripetal displacement rate with the largest deformations on the southern flank of Mt. Epomeo (Galvani et al., 2021). This deformation field has been related to a deflating sill-like body, which represents a magmatic reservoir centered below the resurgent block at depth $\sim 2km$ and contracting at a rate of $\sim 10^5 \text{ m}^3/\text{y}$ (Trasatti et al., 2019).
The island is characterized by geothermal activity, primarily occurring in the southwest portion (Chiodini et al., 2004). According to D'Auria et al., (2018) the southwest hydrothermal processes are unrelated to historical seismicity, while earthquakes predominantly affect the northern part, near the town of Casamicciola Terme, at very shallow depths (~500 m). The genesis of earthquakes is probably linked to the dynamic of structural features of the northern part of the island (D'Auria et al., 2018; Paoletti et al., 2013). Carlino et al., (2006) argued that seismicity in the northern sector, correlated with a lower geothermal gradient, shifting the brittle-ductile transition deeper thus favoring the shallow occurrence of earthquakes.

On August 21, 2017, a M_w 3.9 earthquake in Casamicciola (orange star in Fig. 1) triggered landslides (blue stars in Fig.1), collapses (Nappi et al., 2018), and ground shaking with amplitudes reaching almost ~18 cm/s. The scarcity of data, due to a lack of operating accelerometers on the island and saturation effects on the few working velocimeters (Nazeri et al., 2022) has led to controversy regarding the mechanism of the 2017 earthquake. Braun et al., (2018) proposed a normal faulting event triggering a shallow underground collapse to explain the 4 cm subsidence observed immediately after the earthquake (De Novellis et al., 2018). According to Trasatti et al., (Trasatti et al., 2019) the normal focal mechanism of the 2017 Casamicciola earthquake (Braun et al., 2018; De Novellis et al., 2018; Nappi et al., 2018) suggests that seismicity is consistent with a deflationary forcing process. Differently, Nazeri et al., (2022) asserted that the earthquake activated a reverse dipping-inward fault, which would be consistent with a resurgence mechanism of Monte Epomeo block. Albano et al., (2018) argued that slope movements partially overlapped the coseismic ground displacement retrieved by InSAR data, which resulted from a combination of fault-slip and surficial sliding induced by seismic shaking, that if not distinguished would lead to an improper definition of the source geometry and an overestimation of the coseismic fault slip. Works based on multitemporal differential interferometry techniques (Beccaro et al., 2021) also highlighted a post-event accelerated subsidence rate that approximately returned to pre-earthquake levels after 6 months from the event.

Recently the historically seismic behavior of the island has been linked to a fault-valve type mechanism. This mechanism is coherent with periodic events of pressurization in the hydrothermal reservoir, driven by self-sealing processes, followed by depressurization episodes associated with ruptures (Calderoni et al., 2019). Self-sealing induces, in fact, an increase in fluid pressure, potentially causing local uplifts. The decrease in fluid pressure within ENE-WSW to E-W striking cracks at Mt Epomeo (789 m a.s.l., Fig. 1) may signify a reduction in fluid pressure within the larger-scale, deep hydrothermal system (Manzo et al., 2006; Sepe et al., 2007), leading to progressive crack closure (Sepe et al., 2007).

Velocity variations measurements at Ischia volcanic complex

Using the three components continuous recordings acquired at IOCA, IMTC and IFOR stations (red triangles in Fig. 1), we construct ambient noise autocorrelations (Lobkis & Weaver, 2003; Poli et al., 2020; Sabra, 2005; N. M. Shapiro & Campillo, 2004) (See Supporting Information, Text S1). The analysis involves 8 years of data, from January 2016 to August 2023. The resulting δv/v for the coda time window 10-30s are reported in Fig. 2 a-c for the three seismic stations on the Ischia Island. The δv/v show periodic annual variations of 0.2% of amplitude, with minima of velocity during wet months (Fig. 2j) (Sens-Schönfelder & Wegler, 2006; Wang et al., 2017). At station IOCA (Fig 2a) we additionally observe a clear velocity drop associated with the 2017 M_w 3.9 Casamicciola earthquake (Albano et al., 2018; Braun et al., 2018; Calderoni et al., 2019) (Fig. 1). A similar drop, albeit less visible, is present at other stations, but it is masked by the seasonal signals (Fig. 2b, c). We also observe that all stations show a generalized velocity increment over the full study time (Fig. 2). A similarly imbricated δv/v, with seasonal, earthquakes induced, and long-term velocity changes is observed for other coda time windows (Fig 2d-f,2g-i). In previous studies[14] based on theoretical findings[57], the coda lapse-time-dependent analysis has been designed to retrieve the behavior of velocity variations as function of relative depth. We evaluated the sensitivity of the scattered body waves by considering a 3D sensitivity kernel formulation (Pacheco & Snieder, 2005) (see Supporting Information, Text S2 and Fig. S1). Velocity variations are sensitive approximately to the first 2 km of the crust, whose brittle layer in Ischia Island is extremely thin (Carlino et al., 2006).

To discern the various components of the δv/v time series (see Fig. 2), we developed a comprehensive model, accounting for velocity variations induced by the 2017 Mw3.9 Casamicciola earthquake (Bonilla et al., 2019; Boschelli et al., 2021; Chaves & Schwartz, 2016; Poli et al., 2020; Soldati et al., 2019; Taira et al., 2015, 2018; Wu et al., 2016) and its subsequent post-seismic relaxation and fault-healing processes (Brenguier, Campillo, et al., 2008; Li, 2003; Vidale & Li, 2003). The model also incorporates any permanent post-seismic δv/v (Hobiger et al., 2014), seasonal changes (Barajas et al., 2021; Hillers et al., 2015; Mikhael et al., 2024; Poli et al., 2020; Wang et al., 2017), and long-term linear changes (Taira et al., 2018):

$$\frac{\delta v}{v}^{synth}(t) = A + Bt + \left[C_{per} + C\exp\left(-\frac{t-t_{eq}}{D}\right)\right] H(t-t_{eq}) + \mathrm{E}\,[\sin(\mathrm{wt})] + \mathrm{F}\,[\cos(\mathrm{wt})] \quad [1]$$

In the equation 1 the constant A $[\%]$ represents offset, B $[\%/years]$ is the temporal linear trend of velocity changes, C_{per} $[\%]$ is a permanent co-seismic variation of seismic velocity due to the earthquake , C $[\%]$, is a transient co-seismic velocity change due to the earthquake, that is recovered in a characteristic time D $[year]$. E $[\%]$ and F $[\%]$ are annual velocity variations, and w in the sine and cosine terms were fixed to be 2π year^{-1}. $H(t)$ is the Heaviside step function and t_{eq} is the occurrence time of the earthquake; t is an elapsed time $[year]$. We estimate A, B, C_{per}, C, E, F using a nonlinear least squares approach to fit the measured velocity variations (Fig. 2) and provide the 68% confidence bounds on the coefficients, that it is the percentage of values that lie within 1 standard deviation in a normal distribution. The best-fit model is represented as red lines in figure 2, and the resulting coefficients for each station and coda window are summarized in figure 3 and figure S2.

Dynamic response to the Mw 3.9 Casamicciola earthquake

The coefficients C, C_{per} and D are associated with velocity variations and recovery after the shaking induced by the M_w 3.9 Casamicciola event (Albano et al., 2018; Braun et al., 2018; Calderoni et al., 2019; Nappi et al., 2018; Nazeri et al., 2022). C and C_{per} represent the coseismic velocity drop and its non-recovered amount (C_{per}) and reveal a systematic variation across the study area (Fig. 4 a-c). The largest negative velocity changes are induced at IOCA station which is $\sim 1\ km$ far from the earthquake epicenter (Fig. 3g). Here, nearly all the co-seismic drop is permanent, and it is maximal for the early coda window, reducing at later lapse time, indicating larger damage close to the free surface (Obermann et al., 2013; Poli et al., 2020). The large and permanent velocity changes at the free surface reflect the significant damage of the shallow rocks, interested by several landslides which occurred in response to the M_w 3.9 earthquake (Nappi et al., 2018). At the other two stations the cosesmic drop if fully recovered in 1-2 yrs (Fig. 3c) but is still significantly large (about 0.2%) for such a small magnitude earthquake (Taira et al., 2018). At station IFOR, located in the southern part of the island, we again observe a depth dependence of the coseismic drop (Poli et al., 2020), highlighting largest damage due to the presence of less consolidate shallow rocks (Foda & Chang, 1995; Nardone et al., 2023).

The dynamic strain sensitivity (β, for the complete derivation of the dynamic strain sensitivity see Supporting Information, Text S3, Eq. A.1) is negative at all the 3 sites, as observed on rock samples in laboratory (Renaud et al., 2012) and widely elsewhere (Hillers et al., 2019; Poli et al., 2020; Takano et al., 2019). The strain sensitivity computed from dynamic strain induced by the magnitude Mw 3.9 event in 2017 is~ 10 at IMTC (green) and IOCA (blue, Fig. 3d). The behavior at both sites is not far than co-seismic response in L'Aquila to the Mw 6.2 earthquake (Poli et al., 2020), where dynamic strain sensitivity is in the order ~ 10 but for larger dynamic strains, and, as well, in Turkey (Muller et al., 2023), where in a higher frequency band (2-4Hz) a coseismic seismic velocity drop equal to -1.79% has been observed in response to the M w 7.8 earthquake. Besides, the above-mentioned cases are one order larger than estimates in geothermal areas (Taira et al., 2018). On the other hand, the strain sensitivity is even larger $(\text{in the order} \sim 10^2)$ in the site of IFOR (red, Fig. 3d), in the most south part of the island, where geothermal activity is more intense and it has caused in the past wells explosion, as also retrieved in local seismic records (D'Auria et al., 2018). The observed strong coseismic velocity reductions at IFOR, in the southern part, mirror indeed the major presence of pressurized volcanic fluids in this sector of the island (Brenguier et al., 2014) . It is well known, in fact, that the sensitivity of the seismic velocity to stress changes in the rock increases with decreasing effective pressure (S. A. Shapiro, 2003) and that in volcanic region the effective pressure in the crust can be reduced because of the presence of highly pressurized hydrothermal and magmatic volcanic fluids at depth (Brenguier et al., 2014). In other words, our results on the dynamic strain sensitivity disclose the different levels of pressurization of the hydrothermal fluids circulating in the Ischia Island, responsible for a spatially heterogeneous seismic velocity susceptibility to dynamic stress.

Long term velocity variations and volcanic deformation

The parameter B in Eq. 1 describes the long-term linear trend, which is positive at IOCA and IFOR stations, for all coda lapse time, suggesting a stable velocity increment occurring over a range of depth of several kilometers (Poli et al., 2020), while less resolved is the increment for station IMTC (Fig. 3e). Velocity increment in volcanic systems have been observed as results of strain decreases (compression) during dike intrusions (Donaldson et al., 2019), while stable velocity increases have been interpreted as resulting from pore pressure reduction in geothermal systems (Taira et al., 2018).

To gain more insights about the origin of the observed long-term increment, we estimate the strain evolution (see Supporting Information, Text S4) using GNSS data (dark cyan and cornflower squares in Fig. 1). Horizontal strains are in the order 10^{-5} with a negative trend (Fig. 4), associated with the progressive contraction of the caldera (Trasatti et al., 2019). The strain rate shows a significant heterogeneous variation over the island, with larger values in the northernmost part of the island, in agreement with previous studies (Sepe et al., 2007). From the comparison of the linear trends in the seismic wave velocity variations and in the strain computed in the nearest triad of GPS stations to the velocimeter, we computed the quasi-static strain sensitivity retrieving a value $\sim -10^{2}$ (Fig. 3f) for IFOR and IOCA, slightly smaller at IMTC and null in the first time-lapse window (10-30s).

Discussion

Our long-term (6.7 years) geodetic modeling reveals a generalized contraction of the Ischia Caldera, also reported in previous studies (Galvani et al., 2021; Sepe et al., 2007; Trasatti et al., 2019). Several mechanisms have been proposed to explain the observed contraction and related to the seismic activity in the northern part of the Island. Galvani et al. (Galvani et al., 2021) proposed a deep (4km) contraction of a magmatic reservoir, which feed the shallow faults systems with geothermal fluids. In this model the seismicity is controlled by rise in fluid pressure(Calderoni et al., 2019). On the other hand, Sepe et al. (Sepe et al., 2007) modeled the subsidence and contraction with a crack closure mechanism due to depressurization of shallow faults, through the CO_2 degassing. In this second model, the seismicity in the northern part of the island is mainly controlled by tectonic stressing (Braun et al., 2018). Trasatti et al., (Trasatti et al., 2019) modeled a shallow cooling magma body, around 2 km of depth, plus a creeping fault in the NW part of the island. Their model predicts that degassing and cooling control the subsidence at Ischia and induce creep and related earthquakes in the faults located in the NW part of the island.

With our results we additionally highlight a systematic long-term increment of velocity across all coda window (Fig. 3e), which suggest that both surface and body wave speed increases during the study period (Obermann et al., 2013). The velocity increment can help us to better constrain the mechanism of deformation for the Ischia Caldera (Caudron et al., 2022; Duputel et al., 2009; Makus et al., 2023; Rivet et al., 2014). An increment (decrease) of velocity can be associated with crack closure (opening) and reduction (increment) of pore pressure (Taira et al., 2018; Takano et al., 2017). Thus, any increment in pore pressure in the shallow fault system (Galvani et al., 2021) would manifest in our δv/v, at least for the early coda window. On the other hand, our results (Fig. 3e) better agree with a depressurization of the shallow hydrothermal system, through degassing along faults (Sepe et al., 2007) or sills (Trasatti et al., 2019). The δv/v rate varies across the island, with faster increment rate recorded at IOCA, where largest strain rates are also observed (Fig. 4, (Trasatti et al., 2019)). Our results thus highlight an heterogenous shallow degassing, with mostly effective in the northern part of the Island, and might play a significant role in controlling the aseismic deformation of the Casamicciola faults (Trasatti et al., 2019)

Together with the long-term velocity increment we report significant velocity drops induced by the M_w 3.9 Casamicciola earthquake (Fig. 3 a, b), which exceed the ones observed in regular tectonic environments (Chaves & Schwartz, 2016; Poli et al., 2020; Wu et al., 2016). The combination of a shallow rupture and the action of trapping geological structures(Nazeri & Zollo, 2023) as the volcanic deposits (Foda & Chang, 1995; Nazeri et al., 2022), operating as low-velocity waveguides, caused the amplification of the ground shaking for this moderate earthquake. The largest and permanent velocity changes observed close to the epicenter track the significant shallow damage induced by the earthquakes, including landslides (Albano et al., 2018; Marc et al., 2021; Nappi et al., 2018). The strain sensitivity to the dynamic perturbation (Eq. A.2, Fig. 3f), at IOCA, is in line with previous studies (Poli et al., 2020; Taira et al., 2018), while anomalous values are observed close to the IFOR station (Fig. 3f). In this zone, the lower strain rates we observe (Fig. 3g) indicate slower depressurization and related crack closure, leaving higher pore pressure in shallow rocks, which enhance the sensitivity to dynamic strain perturbation (Poli et al., 2020; Taira et al., 2018). This last observation agrees with previous report of geothermal wells explosion in this part of the island (D'Auria et al., 2018). 0.138

We additionally calculate the strain sensitivity (see Supporting Information, Text S4) using the long-term strain rates (Fig. 3g, 4) and velocity increments (Fig. 3e) for the quasi-static case. The results (Fig. 3f) reveal near zero values in the central part of the island (station IMTC), while remarkable similar large values of the strain sensitivity are observed at IOCA and IFOR. The different response for dynamic (Fig. 3d) and quasi-static (Fig. 3f) deformation suggest the existence of different mechanisms controlling the velocity changes at different frequencies (Rivière et al., 2016).

Conclusion

Our integrated geophysical characterization of the deformation processes at Ischia Island revealed the power of including multiple techniques to deepen our understanding of the dynamic of magmatic systems (as previously experimented in multi-parametric studies (Cabrera-Pérez et al., 2023; Caudron et al., 2021, 2022; Cubuk-Sabuncu et al., 2021; Donaldson et al., 2017, 2019; Olivier et al., 2019; Rivet et al., 2014)). The synergy of geodetic methods and ambient noise monitoring has unveiled a noteworthy sensitivity of δv/v to depressurization processes. This discovery holds promising implications for the potential application of monitoring geothermal production, presenting a valuable avenue for further exploration and utilization.

Data availability

Seismic data are available from the FDSN webservice of the Italian National Institute of Geophysics and Volcanology – INGV (http://webservices.ingv.it/fdsnws/dataselect/1/). GPS data of the station ISC1 are from GNSS Campania network (http://gps.sit.regione.campania.it/). Rain data at pluviometric station of Forio have been downloaded at https://centrofunzionale.regione.campania.it.

Acknowledgement

Authors are grateful to personnel involved in the maintenance of the seismic and geodetic monitoring at Osservatorio Vesuviano, GNSS Campania network, Protezione Civile Regione Campania. Authors also acknowledge Prospero De Martino (Osservatorio Vesuviano, INGV) to provide the time series of GPS data of the NeVocGPS network, Antonella Bobbio (Osservatorio Vesuviano, INGV) to provide the missing data at the seismological stations, Qingyu Wang for sharing her wealth of knowledge on depth sensitivity kernel. Figures were produced with the GMT software package (The Generic Mapping Tools (generic-mapping-tools.org)) and MATLAB Version: 9.13.0 (R2022b) Update 2 (MATLAB Home - MATLAB & Simulink (mathworks.com)). Analysis was done in MATLAB and Python (http://www.python.org). ST was supported by MYBURP Pianeta Dinamico Project (Ministry of University and Research – Fund for Investments of Central Administrations).

Supporting information

Further details on the method used and additional figures are available in the supporting information.

FIGURES

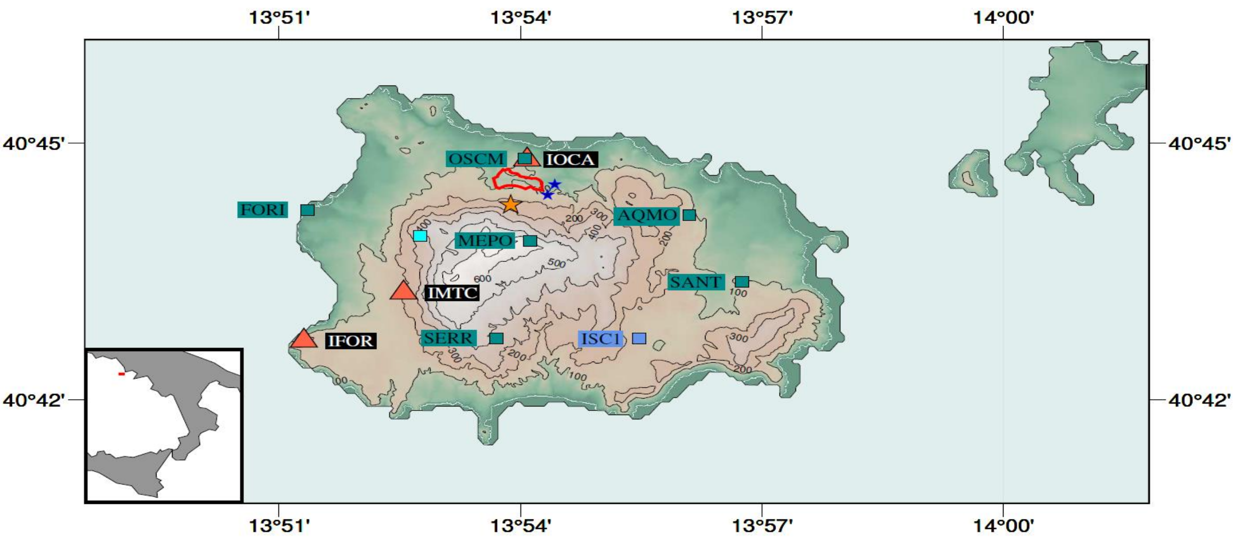

Figure 1 ***Map of the study area****. The red triangles indicate the location of the seismic stations, while the darkcyan squares represents the GPS station of the NeVoCGPS network (Osservatorio Vesuviano) and the cornflower square the GPS station of the GNSS Campania network. The orange star indicates the epicenter of the 21st august 2017, Ischia Earhquake, cyan square represents the pluviometric station of Forio, while the blue stars indicate documented landslides* (Nappi et al., 2018)*. The red line encloses the area most damaged by the earthquake (also called "red zone",* (Azzaro et al., 2017)*. The inset shows the location of the study area (red rectangle) in Italy.*

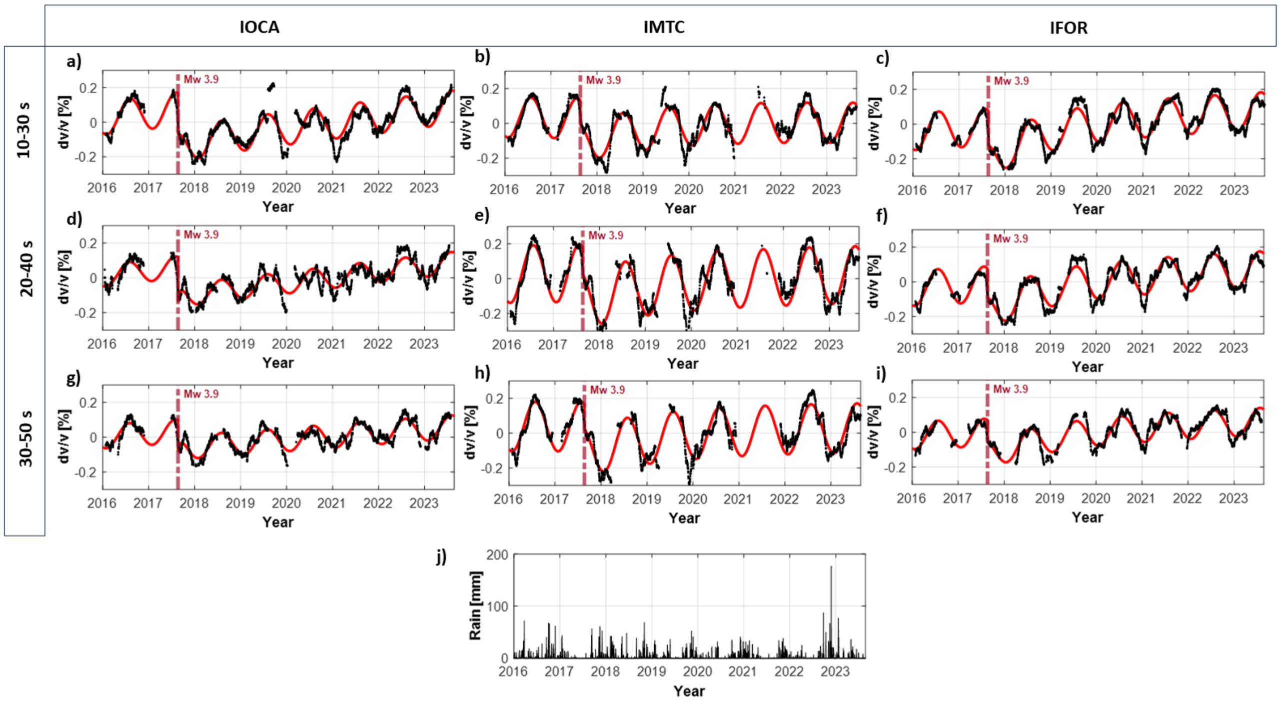

Figure 2 ***– Time Series of Seismological Observations and Rain**: **a)-i)** velocity variations for coda waves time lapse using empirical Green's functions reconstructed by autocorrelation of seismic noise in the frequency band from 0.5 Hz to 1 Hz, for the station IOCA, IMTC and IFOR and using different coda time lapse for analysis (indicated on the left side of the figure). The vertical dashed line highlights the occurrence of Mw 3.9 Ischia earthquake, red line represents the result of fit of equation (1). In **j)** there is the time series of Rain recorded at pluviometric station of Forio (cyan square in fig. 1).*

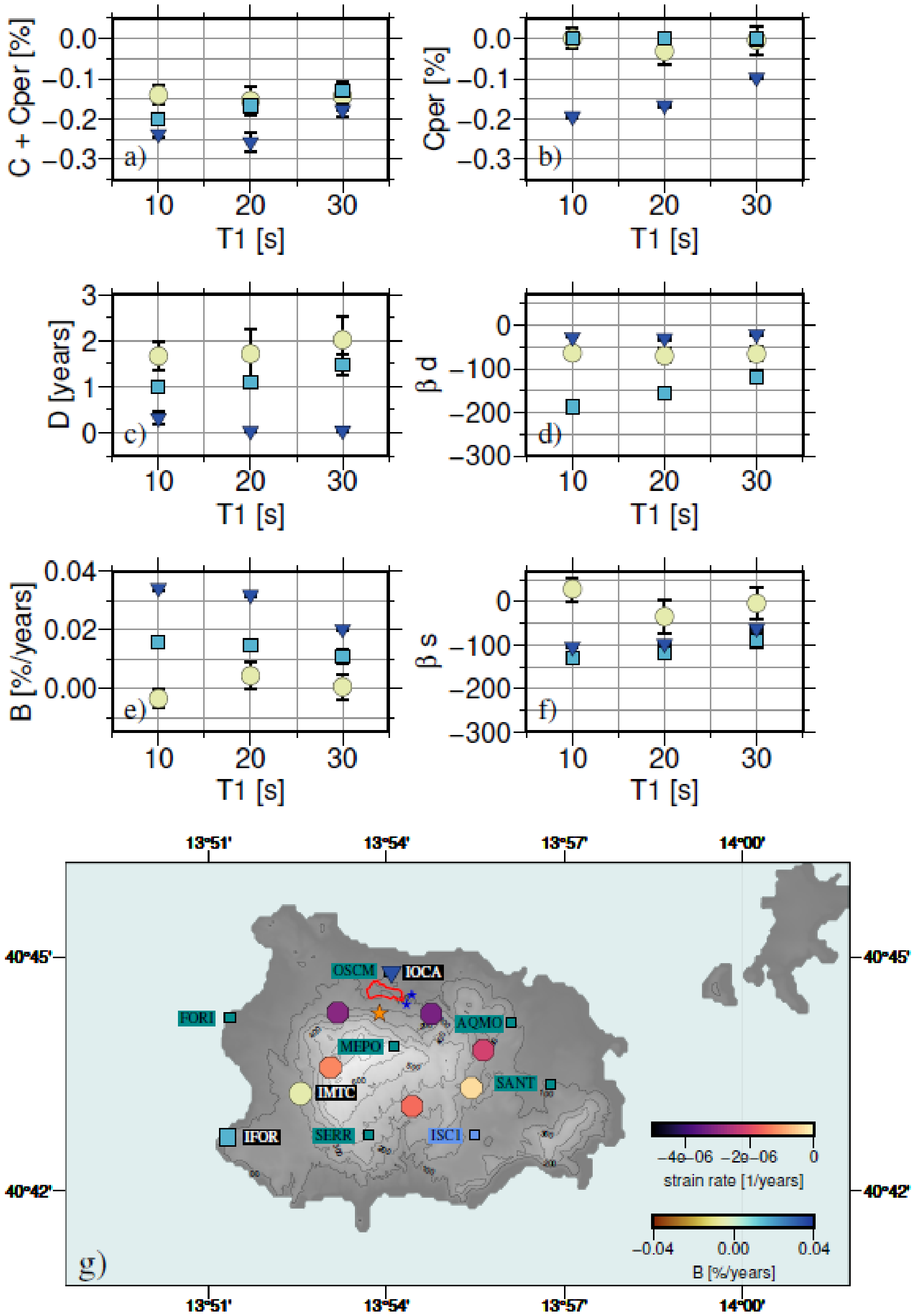

Figure 3 – ***Summary of Results for different Coda Time Lapse at the seismological stations.*** *IOCA is represented by triangles, IMTC by circles and IFOR by squares**: a)** Global Velocity Drops; **b)** Permanent velocity drop; **c)** Recovery time; **d)** dynamic strain sensitivity of velocity variations; **e)** linear trend; **f)** static strain sensitivity of velocity variations; **g)** map view of strain rate (octagons) obtained from slopes of strain vs time curves in Fig 3b and linear trend (coefficient B, symbols ad in the panels a-f)).*

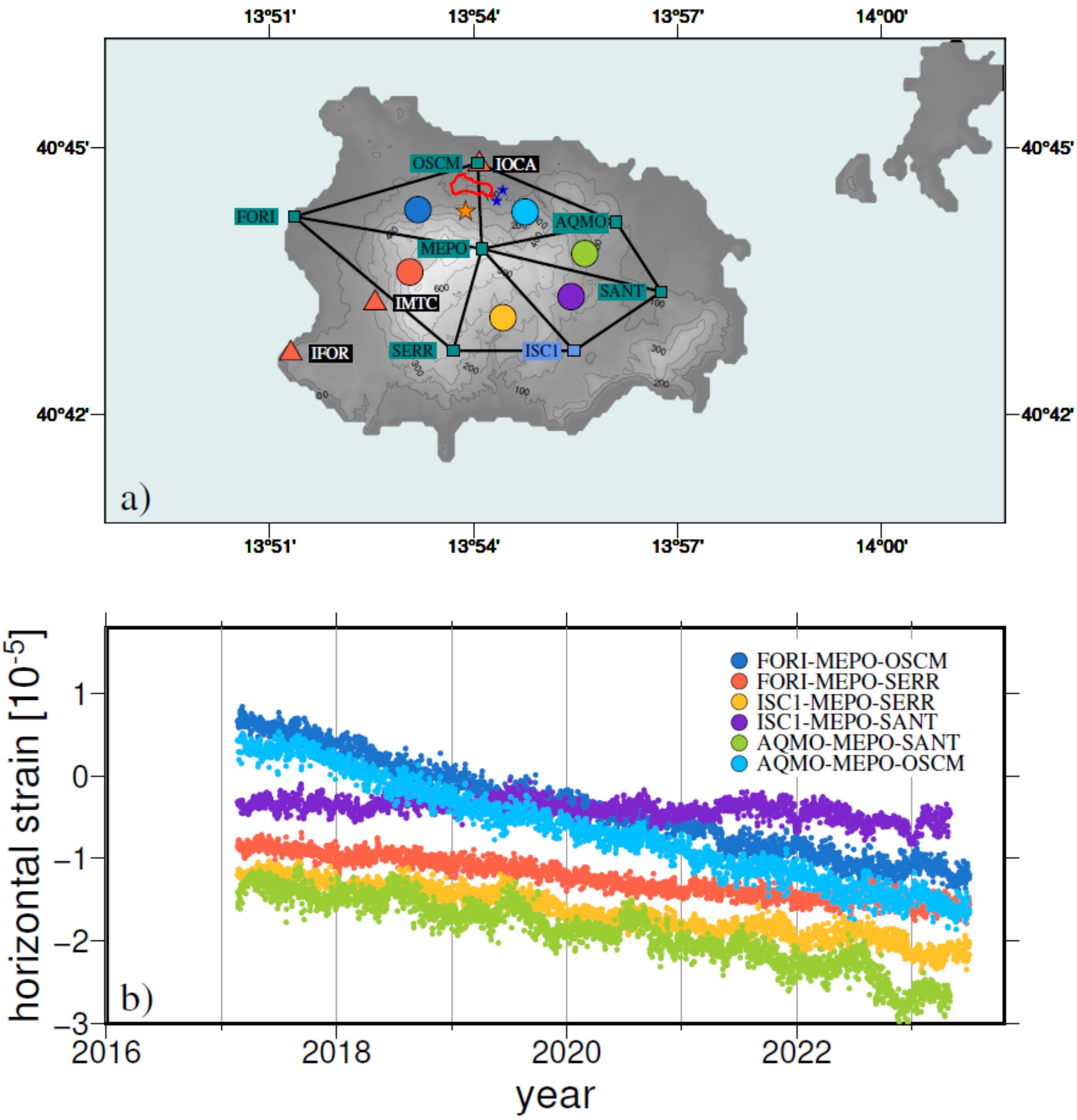

Figure 4 ***Time series of horizontal strain: a)*** *triangles represent seismic station, cornflower and darkcyan squares are GPS station as in fig. 1, circles represent the centroid of the triads of stations (black lines) used to compute the temporal evolution of strain represented in* ***b).***

Reference

Albano, M., Saroli, M., Montuori, A., Bignami, C., Tolomei, C., Polcari, M., Pezzo, G., Moro, M., Atzori, S., Stramondo, S., & Salvi, S. (2018). The Relationship between InSAR Coseismic Deformation and Earthquake-Induced Landslides Associated with the 2017 Mw 3.9 Ischia (Italy) Earthquake. *Geosciences*, *8*(8), 303. https://doi.org/10.3390/geosciences8080303

Azzaro, R., Tertulliani, A., Del Mese, S., Graziani, L., Maramai, A., Martini, G., Paolini, S., Screpanti, A., Verrubbi, V., & Arcoraci, L. (2017). *QUEST - Rilievo macrosismico per il terremoto dell'isola di Ischia del 21 agosto 2017. Rapporto finale*.

Barajas, A., Poli, P., D’Agostino, N., Margerin, L., & Campillo, M. (2021). Separation of Poroelastic and Elastic Processes of an Aquifer From Tectonic Phenomena Using Geodetic, Seismic, and Meteorological Data in the Pollino Region, Italy. *Geochemistry, Geophysics, Geosystems*, *22*(11). https://doi.org/10.1029/2021GC009742

Beccaro, L., Tolomei, C., Gianardi, R., Sepe, V., Bisson, M., Colini, L., De Ritis, R., & Spinetti, C. (2021). Multitemporal and Multisensor InSAR Analysis for Ground Displacement Field Assessment at Ischia Volcanic Island (Italy). *Remote Sensing*, *13*(21), 4253. https://doi.org/10.3390/rs13214253

Bonilla, L. F., Guéguen, P., & Ben-Zion, Y. (2019). Monitoring Coseismic Temporal Changes of Shallow Material during Strong Ground Motion with Interferometry and Autocorrelation. *Bulletin of the Seismological Society of America*, *109*(1), 187–198. https://doi.org/10.1785/0120180092

Boschelli, J., Moschetti, M. P., & Sens-Schönfelder, C. (2021). Temporal Seismic Velocity Variations: Recovery Following From the 2019 M_{w} 7.1 Ridgecrest, California Earthquake. *Journal of Geophysical Research: Solid Earth*, *126*(4). https://doi.org/10.1029/2020JB021465

Braun, T., Famiani, D., & Cesca, S. (2018). Seismological Constraints on the Source Mechanism of the Damaging Seismic Event of 21 August 2017 on Ischia Island (Southern Italy). *Seismological Research Letters*, *89*(5), 1741–1749. https://doi.org/10.1785/0220170274

Brenguier, F., Campillo, M., Hadziioannou, C., Shapiro, N. M., Nadeau, R. M., & Larose, E. (2008). Postseismic Relaxation Along the San Andreas Fault at Parkfield from Continuous Seismological Observations. *Science*, *321*(5895), 1478–1481. https://doi.org/10.1126/science.1160943

Brenguier, F., Campillo, M., Takeda, T., Aoki, Y., Shapiro, N. M., Briand, X., Emoto, K., & Miyake, H. (2014). Mapping pressurized volcanic fluids from induced crustal seismic velocity drops. *Science*, *345*(6192), 80–82. https://doi.org/10.1126/science.1254073

Brenguier, F., Rivet, D., Obermann, A., Nakata, N., Boué, P., Lecocq, T., Campillo, M., & Shapiro, N. (2016). 4-D noise-based seismology at volcanoes: Ongoing efforts and perspectives. *Journal of Volcanology and Geothermal Research*, *321*, 182–195. https://doi.org/10.1016/j.jvolgeores.2016.04.036

Brenguier, F., Shapiro, N. M., Campillo, M., Ferrazzini, V., Duputel, Z., Coutant, O., & Nercessian, A. (2008). Towards forecasting volcanic eruptions using seismic noise. *Nature Geoscience*, *1*(2), 126–130. https://doi.org/10.1038/ngeo104

Cabrera-Pérez, I., D’Auria, L., Soubestre, J., Przeor, M., Barrancos, J., García-Hernández, R., Ibáñez, J. M., Koulakov, I., van Dorth, D. M., Ortega, V., Padilla, G. D., Sagiya, T., & Pérez, N. (2023). Spatio-temporal velocity variations observed during the pre-eruptive episode of La Palma 2021 eruption inferred from ambient noise interferometry. *Scientific Reports*, *13*(1), 12039. https://doi.org/10.1038/s41598-023-39237-9

Calderoni, G., Di Giovambattista, R., Pezzo, G., Albano, M., Atzori, S., Tolomei, C., & Ventura, G. (2019). Seismic and Geodetic Evidences of a Hydrothermal Source in the Md 4.0, 2017, Ischia

Earthquake (Italy). *Journal of Geophysical Research: Solid Earth*, *124*(5), 5014–5029. https://doi.org/10.1029/2018JB016431

Caricchi, L., Townsend, M., Rivalta, E., & Namiki, A. (2021). The build-up and triggers of volcanic eruptions. *Nature Reviews Earth & Environment*, *2*(7), 458–476. https://doi.org/10.1038/s43017-021-00174-8

Carlino, S., Cubellis, E., Luongo, G., & Obrizzo, F. (2006). On the mechanics of caldera resurgence of Ischia Island (southern Italy). *Geological Society, London, Special Publications*, *269*(1), 181–193. https://doi.org/10.1144/GSL.SP.2006.269.01.12

Caudron, C., Aoki, Y., Lecocq, T., De Plaen, R., Soubestre, J., Mordret, A., Seydoux, L., & Terakawa, T. (2022). Hidden pressurized fluids prior to the 2014 phreatic eruption at Mt Ontake. *Nature Communications*, *13*(1), 6145. https://doi.org/10.1038/s41467-022-32252-w

Caudron, C., Girona, T., Jolly, A., Christenson, B., Savage, M. K., Carniel, R., Lecocq, T., Kennedy, B., Lokmer, I., Yates, A., Hamling, I., Park, I., Kilgour, G., & Mazot, A. (2021). A quest for unrest in multiparameter observations at Whakaari/White Island volcano, New Zealand 2007–2018. *Earth, Planets and Space*, *73*(1), 195. https://doi.org/10.1186/s40623-021-01506-0

Chaves, E. J., & Schwartz, S. Y. (2016). Monitoring transient changes within overpressured regions of subduction zones using ambient seismic noise. *Science Advances*, *2*(1). https://doi.org/10.1126/sciadv.1501289

Civetta, L., Gallo, G., & Orsi, G. (1991). Sr- and Nd-isotope and trace-element constraints on the chemical evolution of the magmatic system of Ischia (Italy) in the last 55 ka. *Journal of Volcanology and Geothermal Research*, *46*(3–4), 213–230. https://doi.org/10.1016/0377-0273(91)90084-D

Cubuk-Sabuncu, Y., Jónsdóttir, K., Caudron, C., Lecocq, T., Parks, M. M., Geirsson, H., & Mordret, A. (2021). Temporal Seismic Velocity Changes During the 2020 Rapid Inflation at Mt. Þorbjörn-Svartsengi, Iceland, Using Seismic Ambient Noise. *Geophysical Research Letters*, *48*(11). https://doi.org/10.1029/2020GL092265

D'Auria, L., Giudicepietro, F., Tramelli, A., Ricciolino, P., Bascio, D. Lo, Orazi, M., Martini, M., Peluso, R., Scarpato, G., & Esposito, A. (2018). The Seismicity of Ischia Island. *Seismological Research Letters*, *89*(5), 1750–1760. https://doi.org/10.1785/0220180084

De Martino, P., Dolce, M., Brandi, G., Scarpato, G., & Tammaro, U. (2021). The Ground Deformation History of the Neapolitan Volcanic Area (Campi Flegrei Caldera, Somma–Vesuvius Volcano, and Ischia Island) from 20 Years of Continuous GPS Observations (2000–2019). *Remote Sensing*, *13*(14), 2725. https://doi.org/10.3390/rs13142725

De Novellis, V., Carlino, S., Castaldo, R., Tramelli, A., De Luca, C., Pino, N. A., Pepe, S., Convertito, V., Zinno, I., De Martino, P., Bonano, M., Giudicepietro, F., Casu, F., Macedonio, G., Manunta, M., Cardaci, C., Manzo, M., Di Bucci, D., Solaro, G., … Tizzani, P. (2018). The 21 August 2017 Ischia (Italy) Earthquake Source Model Inferred From Seismological, GPS, and DInSAR Measurements. *Geophysical Research Letters*, *45*(5), 2193–2202. https://doi.org/10.1002/2017GL076336

Delorey, A. A., Guyer, R. A., Bokelmann, G. H. R., & Johnson, P. A. (2021). Probing the Damage Zone at Parkfield. *Geophysical Research Letters*, *48*(13). https://doi.org/10.1029/2021GL093518

Donaldson, C., Caudron, C., Green, R. G., Thelen, W. A., & White, R. S. (2017). Relative seismic velocity variations correlate with deformation at Kīlauea volcano. *Science Advances*, *3*(6). https://doi.org/10.1126/sciadv.1700219

Donaldson, C., Winder, T., Caudron, C., & White, R. S. (2019). Crustal seismic velocity responds to a magmatic intrusion and seasonal loading in Iceland's Northern Volcanic Zone. *Science Advances*, *5*(11). https://doi.org/10.1126/sciadv.aax6642

Duputel, Z., Ferrazzini, V., Brenguier, F., Shapiro, N., Campillo, M., & Nercessian, A. (2009). Real time monitoring of relative velocity changes using ambient seismic noise at the Piton de la Fournaise volcano (La Réunion) from January 2006 to June 2007. *Journal of Volcanology and Geothermal Research*, *184*(1–2), 164–173. https://doi.org/10.1016/j.jvolgeores.2008.11.024

Foda, M. A., & Chang, Y.-H. (1995). Faraday resonance in thin sedimentary layers. *Geophysical Journal International*, *123*(2), 559–571. https://doi.org/10.1111/j.1365-246X.1995.tb06871.x

Galvani, A., Pezzo, G., Sepe, V., & Ventura, G. (2021). Shrinking of Ischia Island (Italy) from Long-Term Geodetic Data: Implications for the Deflation Mechanisms of Resurgent Calderas and Their Relationships with Seismicity. *Remote Sensing*, *13*(22), 4648. https://doi.org/10.3390/rs13224648

Hillers, G., Campillo, M., Brenguier, F., Moreau, L., Agnew, D. C., & Ben-Zion, Y. (2019). Seismic Velocity Change Patterns Along the San Jacinto Fault Zone Following the 2010 *M* 7.2 El Mayor-Cucapah and *M* 5.4 Collins Valley Earthquakes. *Journal of Geophysical Research: Solid Earth*, *124*(7), 7171–7192. https://doi.org/10.1029/2018JB017143

Hillers, G., Retailleau, L., Campillo, M., Inbal, A., Ampuero, J. -P., & Nishimura, T. (2015). In situ observations of velocity changes in response to tidal deformation from analysis of the high-frequency ambient wavefield. *Journal of Geophysical Research: Solid Earth*, *120*(1), 210–225. https://doi.org/10.1002/2014JB011318

Hobiger, M., Wegler, U., Shiomi, K., & Nakahara, H. (2014). Single-station cross-correlation analysis of ambient seismic noise: application to stations in the surroundings of the 2008 Iwate-Miyagi Nairiku earthquake. *Geophysical Journal International*, *198*(1), 90–109. https://doi.org/10.1093/gji/ggu115

Jin, J., Rivière, J., Ohara, Y., & Shokouhi, P. (2018). Dynamic acousto-elastic response of single fatigue cracks with different microstructural features: An experimental investigation. *Journal of Applied Physics*, *124*(7). https://doi.org/10.1063/1.5036531

Li, Y.-G. (2003). Postseismic Fault Healing on the Rupture Zone of the 1999 M 7.1 Hector Mine, California, Earthquake. *Bulletin of the Seismological Society of America*, *93*(2), 854–869. https://doi.org/10.1785/0120020131

Lobkis, O. I., & Weaver, R. L. (2003). Coda-Wave Interferometry in Finite Solids: Recovery of <math display="inline"> <mi>P</mi> </math> -to- <math display="inline"> <mi>S</mi> </math>

Conversion Rates in an Elastodynamic Billiard. *Physical Review Letters*, *90*(25), 254302. https://doi.org/10.1103/PhysRevLett.90.254302

Makus, P., Sens-Schönfelder, C., Illien, L., Walter, T. R., Yates, A., & Tilmann, F. (2023). Deciphering the Whisper of Volcanoes: Monitoring Velocity Changes at Kamchatka's Klyuchevskoy Group With Fluctuating Noise Fields. *Journal of Geophysical Research: Solid Earth*, *128*(4). https://doi.org/10.1029/2022JB025738

Manzo, M., Ricciardi, G. P., Casu, F., Ventura, G., Zeni, G., Borgström, S., Berardino, P., Del Gaudio, C., & Lanari, R. (2006). Surface deformation analysis in the Ischia Island (Italy) based on spaceborne radar interferometry. *Journal of Volcanology and Geothermal Research*, *151*(4), 399–416. https://doi.org/10.1016/j.jvolgeores.2005.09.010

Marc, O., Sens-Schönfelder, C., Illien, L., Meunier, P., Hobiger, M., Sawazaki, K., Rault, C., & Hovius, N. (2021). Toward Using Seismic Interferometry to Quantify Landscape Mechanical Variations after Earthquakes. *Bulletin of the Seismological Society of America*, *111*(3), 1631–1649. https://doi.org/10.1785/0120200264

Mikhael, N., Poli, P., & Garambois, S. (2024). Non-Linear Seismic Velocity Variations Observed During a Seismic Swarm in the Alto Tiberina Low Angle Normal Fault From Ambient Noise Correlation Measurements. *Journal of Geophysical Research: Solid Earth*, *129*(2). https://doi.org/10.1029/2023JB028232

Nappi, R., Alessio, G., Gaudiosi, G., Nave, R., Marotta, E., Siniscalchi, V., Civico, R., Pizzimenti, L., Peluso, R., Belviso, P., & Porfido, S. (2018). The 21 August 2017 Md 4.0 Casamicciola Earthquake: First Evidence of Coseismic Normal Surface Faulting at the Ischia Volcanic Island. *Seismological Research Letters*, *89*(4), 1323–1334. https://doi.org/10.1785/0220180063

Nardone, L., Vassallo, M., Cultrera, G., Sapia, V., Petrosino, S., Pischiutta, M., Di Vito, M., de Vita, S., Galluzzo, D., Milana, G., Bellucci Sessa, E., Bobbio, A., Bordoni, P., Cara, F., Carandente, A., Civico, R., Cogliano, R., Cusano, P., Di Giulio, G., … Tramelli, A. (2023). A geophysical multidisciplinary approach to investigate the shallow subsoil structures in volcanic environment: The case of Ischia Island. *Journal of Volcanology and Geothermal Research*, *438*, 107820. https://doi.org/10.1016/j.jvolgeores.2023.107820

Nazeri, S., & Zollo, A. (2023). EASOt-AP: An open-source MATLAB package to estimate the seismic moment, rupture radius, and stress-drop of earthquakes from time-dependent P-wave displacements. *Computers & Geosciences*, *171*, 105293. https://doi.org/10.1016/j.cageo.2022.105293

Nazeri, S., Zollo, A., Adinolfi, G. M., Amoroso, O., & Picozzi, M. (2022). The 2017 Ischia Earthquake (Southern Italy): Source Mechanism and Rupture Model From the Inversion of a Near-Source Strong Motion Record. *IEEE Transactions on Geoscience and Remote Sensing*, *60*, 1–10. https://doi.org/10.1109/TGRS.2021.3111400

Obermann, A., Planès, T., Larose, E., Sens-Schönfelder, C., & Campillo, M. (2013). Depth sensitivity of seismic coda waves to velocity perturbations in an elastic heterogeneous medium. *Geophysical Journal International*, *194*(1), 372–382. https://doi.org/10.1093/gji/ggt043

Olivier, G., Brenguier, F., Carey, R., Okubo, P., & Donaldson, C. (2019). Decrease in Seismic Velocity Observed Prior to the 2018 Eruption of Kīlauea Volcano With Ambient Seismic Noise Interferometry. *Geophysical Research Letters*, *46*(7), 3734–3744. https://doi.org/10.1029/2018GL081609

Ostrovsky, L. A., & Johnson, P. A. (2001). Dynamic nonlinear elasticity in geomaterials. *La Rivista Del Nuovo Cimento*, *24*(7), 1–46. https://doi.org/10.1007/BF03548898

Pacheco, C., & Snieder, R. (2005). Time-lapse travel time change of multiply scattered acoustic waves. *The Journal of the Acoustical Society of America*, *118*(3), 1300–1310. https://doi.org/10.1121/1.2000827

Paoletti, V., D'Antonio, M., & Rapolla, A. (2013). The structural setting of the Ischia Island (Phlegrean Volcanic District, Southern Italy): Inferences from geophysics and geochemistry. *Journal of Volcanology and Geothermal Research*, *249*, 155–173. https://doi.org/10.1016/j.jvolgeores.2012.10.002

Poli, P., Marguin, V., Wang, Q., D'Agostino, N., & Johnson, P. (2020). Seasonal and Coseismic Velocity Variation in the Region of L'Aquila From Single Station Measurements and Implications for Crustal Rheology. *Journal of Geophysical Research: Solid Earth*, *125*(7), e2019JB019316. https://doi.org/10.1029/2019JB019316

Renaud, G., Le Bas, P.-Y., & Johnson, P. A. (2012). Revealing highly complex elastic nonlinear (anelastic) behavior of Earth materials applying a new probe: Dynamic acoustoelastic testing. *Journal of Geophysical Research: Solid Earth*, *117*(B6), n/a-n/a. https://doi.org/10.1029/2011JB009127

Rivet, D., Brenguier, F., Clarke, D., Shapiro, N. M., & Peltier, A. (2014). Long-term dynamics of Piton de la Fournaise volcano from 13 years of seismic velocity change measurements and GPS observations. *Journal of Geophysical Research: Solid Earth*, *119*(10), 7654–7666. https://doi.org/10.1002/2014JB011307

Rivière, J., Pimienta, L., Scuderi, M., Candela, T., Shokouhi, P., Fortin, J., Schubnel, A., Marone, C., & Johnson, P. A. (2016). Frequency, pressure, and strain dependence of nonlinear elasticity in Berea Sandstone. *Geophysical Research Letters*, *43*(7), 3226–3236. https://doi.org/10.1002/2016GL068061

Sabra, K. G. (2005). Extracting time-domain Green's function estimates from ambient seismic noise. *Geophysical Research Letters*, *32*(3), L03310. https://doi.org/10.1029/2004GL021862

Segall, P. (2013). Volcano deformation and eruption forecasting. *Geological Society, London, Special Publications*, *380*(1), 85–106. https://doi.org/10.1144/SP380.4

Sens-Schönfelder, C., & Wegler, U. (2006). Passive image interferometry and seasonal variations of seismic velocities at Merapi Volcano, Indonesia. *Geophysical Research Letters*, *33*(21), L21302. https://doi.org/10.1029/2006GL027797

Sepe, V., Atzori, S., & Ventura, G. (2007). Subsidence due to crack closure and depressurization of hydrothermal systems: a case study from Mt Epomeo (Ischia Island, Italy). *Terra Nova*, *19*(2), 127–132. https://doi.org/10.1111/j.1365-3121.2006.00727.x

Shapiro, N. M., & Campillo, M. (2004). Emergence of broadband Rayleigh waves from correlations of the ambient seismic noise. *Geophysical Research Letters*, *31*(7), n/a-n/a. https://doi.org/10.1029/2004GL019491

Shapiro, S. A. (2003). Elastic piezosensitivity of porous and fractured rocks. *GEOPHYSICS*, *68*(2), 482–486. https://doi.org/10.1190/1.1567215

Snieder, R., & Hagerty, M. (2004). Monitoring change in volcanic interiors using coda wave interferometry: Application to Arenal Volcano, Costa Rica. *Geophysical Research Letters*, *31*(9). https://doi.org/10.1029/2004GL019670

Soldati, G., Zaccarelli, L., & Faenza, L. (2019). Spatio-temporal seismic velocity variations associated to the 2016–2017 central Italy seismic sequence from noise cross-correlation. *Geophysical Journal International*, *219*(3), 2165–2173. https://doi.org/10.1093/gji/ggz429

Taira, T., Brenguier, F., & Kong, Q. (2015). Ambient noise-based monitoring of seismic velocity changes associated with the 2014 M_w 6.0 South Napa earthquake. *Geophysical Research Letters*, *42*(17), 6997–7004. https://doi.org/10.1002/2015GL065308

Taira, T., Nayak, A., Brenguier, F., & Manga, M. (2018). Monitoring reservoir response to earthquakes and fluid extraction, Salton Sea geothermal field, California. *Science Advances*, *4*(1). https://doi.org/10.1126/sciadv.1701536

Takano, T., Nishimura, T., & Nakahara, H. (2017). Seismic velocity changes concentrated at the shallow structure as inferred from correlation analyses of ambient noise during volcano deformation at Izu-Oshima, Japan. *Journal of Geophysical Research: Solid Earth*, *122*(8), 6721–6736. https://doi.org/10.1002/2017JB014340

Takano, T., Nishimura, T., Nakahara, H., Ueda, H., & Fujita, E. (2019). Sensitivity of Seismic Velocity Changes to the Tidal Strain at Different Lapse Times: Data Analyses of a Small Seismic Array at Izu-Oshima Volcano. *Journal of Geophysical Research: Solid Earth*, *124*(3), 3011–3023. https://doi.org/10.1029/2018JB016235

Townsend, M. (2022). Linking surface deformation to thermal and mechanical magma chamber processes. *Earth and Planetary Science Letters*, *577*, 117272. https://doi.org/10.1016/j.epsl.2021.117272

Trasatti, E., Acocella, V., Di Vito, M. A., Del Gaudio, C., Weber, G., Aquino, I., Caliro, S., Chiodini, G., de Vita, S., Ricco, C., & Caricchi, L. (2019). Magma Degassing as a Source of Long-Term Seismicity at Volcanoes: The Ischia Island (Italy) Case. *Geophysical Research Letters*, *46*(24), 14421–14429. https://doi.org/10.1029/2019GL085371

Vidale, J. E., & Li, Y.-G. (2003). Damage to the shallow Landers fault from the nearby Hector Mine earthquake. *Nature*, *421*(6922), 524–526. https://doi.org/10.1038/nature01354

Wang, Q.-Y., Brenguier, F., Campillo, M., Lecointre, A., Takeda, T., & Aoki, Y. (2017). Seasonal Crustal Seismic Velocity Changes Throughout Japan. *Journal of Geophysical Research: Solid Earth*, *122*(10), 7987–8002. https://doi.org/10.1002/2017JB014307

Wu, C., Delorey, A., Brenguier, F., Hadziioannou, C., Daub, E. G., & Johnson, P. (2016). Constraining depth range of *S* wave velocity decrease after large earthquakes near Parkfield, California. *Geophysical Research Letters*, *43*(12), 6129–6136. https://doi.org/10.1002/2016GL069145